Film and Line Tension Effects on the Attachment of Particles to an Interface

IV. Experimental Studies with Bubbles in Solutions of Dodecyl Sodium Sulfate

PETER ATANASSOV KRALCHEVSKY, ALEXANDER DUSHKOV NIKOLOV, AND IVAN BOYANOV IVANOV[1]

Laboratory of Thermodynamics and Physicochemical Hydrodynamics, Faculty of Chemistry, University of Sofia, 1126 Sofia, Bulgaria

Received April 23, 1984; accepted August 15, 1985

The film and line tensions appearing when a bubble is pressed against a liquid–gas interface are measured with solutions of dodecyl sodium sulfate at two electrolyte concentrations. A strong dependence of the film and line tensions on the system geometrical parameters is found. The measured values of the line tension are in agreement with the experimental results of S. Torza and G. Mason (*Kolloid-Z. Z. Polym.* **246,** 593, 1971) and the theory of N. V. Churaev *et al.* (*Kolloidn. Zh.* **42,** 703, 1980; *J. Colloid Interface Sci.* **89,** 16, 1982) but are different from those of D. Platikanov *et al.* (*J. Colloid Interface Sci.* **75,** 612, 620, 1980), and A. Scheludko *et al.* (*in* "The Modern Theory of Capillarity" (F. C. Goodrich and A. Rusanov, Eds.), Akademie-Verlag, Berlin, 1981).

1. INTRODUCTION

The methods, developed in the previous parts of this series (7–9) are used now for determining the film and line tensions when liquid films are formed between small air bubbles pressed against a liquid/air flat interface by the buoyancy force. The experimental method we used is essentially the "shrinking bubble method" of Princen and Mason (10): a relatively large bubble at the liquid surface is let to decrease gradually its volume due to the escaping gas through the thin film and its geometrical parameters are recorded optically as functions of the time. The main advantage of this method is that it allows changing some of the system parameters, keeping the others (temperature and concentrations) constant and well-defined. We chose as surfactant the dodecyl sodium sulfate not only because it is readily available in a highly purified form, but also because we wanted to compare our results with the measurements of de Feijter (11) of the tension of planar films and of Scheludko and Platikanov *et al.* (4–6) of the line tension.

The major outcome of our study was the conclusion that both the film and line tensions of very small films depend strongly on the geometrical parameters of the system, so that it is meaningless for these systems to consider the film and line tensions, γ and κ, as functions only of the electrolyte and/or surfactant concentrations. In fact, γ and κ turned out to depend more on the bubble radius than on the composition of the solution. Hence, we worked only with two electrolyte concentrations.

The paper is organized as follows. In Section 2 we describe the apparatus and materials used, the cleaning and purification procedures (extremely important for obtaining reproducible results), and the method by which the values of the radii of the bubble, the contact line, and the film were calculated for a given moment. Section 3 contains a summary of some previously derived formulae (see (7–9)), the

[1] To whom correspondence should be addressed.

0021-9797/86 $3.00

connection between them, and the way they must be used for the calculation of the film and line tension. In Section 4 the experimental results are discussed and analyzed by using the theory of Churaev, Starov, and Derjaguin (2, 3); they are also compared with the measurements of the line tension by Torza and Mason (1) and Scheludko and Platikanov *et al.* The error calculations are described in the Appendix.

2. EXPERIMENTAL PROCEDURE AND MATERIALS

The experiments were carried out with 0.05% (1.73×10^{-3} kmole/m^3) solutions of dodecyl sodium sulfate (Fisher Scientific 0-2674 for high performance liquid chromatography) and two concentrations of NaCl (Merck, analytical grade)—0.25 and 0.32 kmole/m^3. Before use the sodium chloride was heated for several hours at 500°C to remove organic impurities. The solutions were prepared with doubly distilled water with specific conductivity 10^{-4} Ω^{-1} m^{-1} and surface tension 72.4 mN/m. All experiments were carried out in a thermostated room at 22 ± 0.5°C. To check the purity of the dodecyl sodium sulfate we measured the surface tension σ of its solutions at several surfactant concentrations C_s (with 0.32 kmole/m^3 NaCl added) by the Wilhelmy method with scratched plate—the precision of this method is ±0.1 mN/m (12). Since the isotherm σ vs log C_s (Fig. 1) did not exhibit minimum at CMC we concluded that impurities of higher surface activity than the dodecyl sodium sulfate were missing. The surface tensions of the two solutions used, with 0.25 and 0.32 kmole/m^3 NaCl, were 32.4 and 31.7 mN/m, respectively.

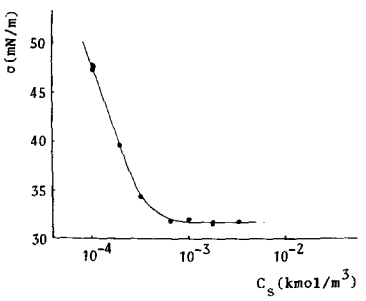

FIG. 1. The isotherm of the surface tension σ vs the surfactant concentration, C_s, of water solutions of dodecyl sodium sulfate with 0.32 kmole/m^3 NaCl added at 22 ± 0.5°C.

The essential part of the measurement cell (the one containing the solution) consists of a glass cylinder of diameter 1 cm and height 1.4 cm whose bottom is an optically plane-parallel glass. The bottom was fixed to the cylinder with glass powder heated at 500°C without using chemical seals. Measurements were taken to allow saturation of the vapors above the solution, to a slightly convex meniscus (to fix the bubble in the center of the cell), and to prevent dust particles and other impurities from reaching the solution. In order to decrease the vibrations the whole system with the microscope was mounted over a 4000-kg antivibrational block. The air bubbles were blown out of a Hamilton syringe. Before each measurement the cell was put for several hours in fresh chromic acid, then rinsed with distilled water and steamed for 30 min. The syringe was rinsed several times with pure ethanol and double distilled water and then boiled in doubly distilled water for an hour.

The optical measurements were carried out with a microscope Epival Interphako (Carl Zeiss, Jena). The initial radius of the bubbles was around 200 μm and measurements of the contact line radius r_c (in reflected light), the bubble radius at the equator R (in transmitted light) and the radius of curvature of the film R_f (by the shearing method) as a function of the time, t, were started after R came down to around 150 μm. (For details on the optical techniques and the methods used for determining R_f see Part III.) The experimental results for Run No. 1a (0.25 kmole/m^3 NaCl) are shown on Fig. 2. The values of r_c and R were recorded visually at the moments when the diameter of the respective circumference was equal to an integer number of scale divisions. At suitably chosen time intervals (100 ÷ 200 s) the image was split and measurements of R_f were performed either by taking photographs (full circles on the curve $R_f(t)$ in Fig.

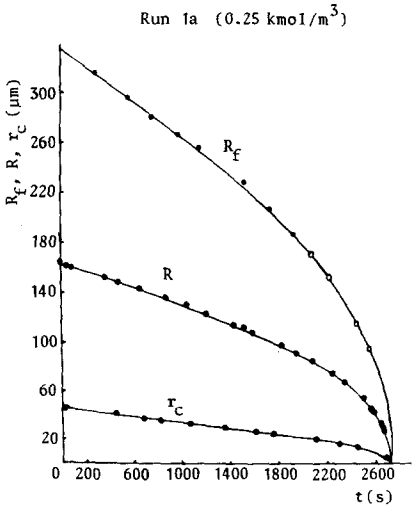

FIG. 2. Dependence of the film, bubble, and contact line radii R_f, R, and r_c on time, t, for Run 1a of a solution of dodecyl sodium sulfate with 0.25 kmole/m^3 NaCl. The curves were calculated by least-squares fitting of the experimental data. Full circles denote values of R_f calculated from photographs and open circles correspond to visual measurements of R_f.

2) or visually, by counting the number of interference rings (open circles on the curve $R_f(t)$). It was possible to measure also r_c from the photographs—these values never differed by more than 0.3 μm from the values determined for the same moment from the interpolation formula (see below).

A major experimental problem is that we need for the calculations the set of values r_c, R, and R_f at a given moment, t, whereas some time elapses after the registration of each of these quantities. One possible issue is to find the sought values by least-squares interpolation of the data for $r_c(t)$, $R(t)$, and $R_f(t)$. This procedure requires, however, a very high precision of the interpolation. All our attempts to achieve it by representing these functions through polynomials failed. Because of that we constructed a more efficient interpolation formula suggested by the following qualitative considerations (see also (10)). The rate dN/dt at which the gas escapes from the bubble can be expressed approximately in two equivalent ways:

$$\frac{dN}{dt} \approx -\frac{P_a}{k_b T}\frac{d}{dt}\left(\tfrac{4}{3}\pi R^3\right) \approx K(\pi r_c^2)\Delta C_g$$

where P_a is the atmospheric pressure, T—temperature, k_b—Boltzmann's constant, K—the film permeability (10), and $C_g = (2\sigma/R)k_bT$ is the difference in concentration of the gas in the two gas phases. Since $r_c \approx R \sin\varphi_c$ (see Fig. 3) and φ_c varies only a little for the whole process, the integral of the above equation can be written in the form $R(t) = a_1(t_0 - t)^{1/2}$. The latter being an approximate formula, we tried to interpolate our experimental data by the more sophisticated and supple expression

$$R(t) = a_1(t_0 - t)^q + a_2(t_0 - t)t, \qquad [1]$$

where t_0, q, a_1, and a_2 are constants to be determined by the minimization of the dispersion

$$\Phi_1(a_1, a_2, t_0, q) = \sum_i [R(t_i) - R_i]^2. \qquad [2]$$

Here R_i is the measured value of R in the moment t_i and $R(t_i)$ is calculated from [1]. The constants a_1 and a_2 are calculated from two of the necessary conditions for minimum of Φ_1:

$$\frac{\partial\Phi_1}{\partial a_1} = 0; \quad \frac{\partial\Phi_1}{\partial a_2} = 0 \qquad [3]$$

and computer minimization of [2] is carried out by variation only of the parameters t_0 and q. The similarity of the experimental dependences $R(t)$, $r_c(t)$, and $R_f(t)$ suggests use of in-

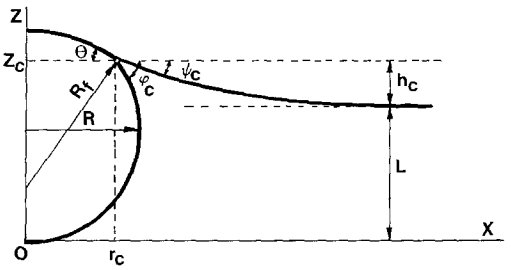

FIG. 3. Scheme of a bubble of equatorial radius R, attached to a liquid surface. R_f and r_c are the radii of curvature of the film and the contact line and θ, φ_c, and ψ_c are the angles at which the film, the lower bubble surface, and the external meniscus meet the plane of the contact line.

terpolation formulae for r_c and R_f similar to [1]:

$$r_c(t) = b_0(t_0 - t)^q + (t_0 - t)(b_1 + b_2 t), \quad [4]$$

$$R_f(t) = c_1(t_0 - t)^q + c_2(t_0 - t)^{q/2} \quad [5]$$

and to construct the respective dispersions $\Phi_2(b_0, b_1, b_2)$ and $\Phi_3(c_1, c_2)$ in the same way as [2]. The constants b_0, b_1, b_2, c_1, c_2 are determined from the same conditions for minimum as [3]. This interpolation procedure gave excellent results: the standard deviations were $\Delta r_c \pm 0.1$, $\Delta R \pm 0.1$, and $\Delta R_f \pm 0.5$ μm for 0.25 kmole/m^3 NaCl and $\Delta R_f \pm 1$ μm for 0.32 kmole/m^3 NaCl.

3. COMPUTATIONAL PROCEDURE

Our final aim is the calculation of the film and line tension γ and κ, respectively, from the experimentally measured values of the solution surface tension σ and the radii r_c, R, and R_f. This will be done by using the force balance equations (Eqs. [15] and [16] of Part I, Ref. (7), with $\sigma_{12} = \sigma_{23} = \sigma$ and $\sigma_{13} = \gamma$):

$$\gamma/\sigma = (\sin \varphi_c + \sin \psi_c)/\sin \theta, \quad [6]$$

$$\kappa/\sigma = r_c[\cos \varphi_c + \cos \psi_c - (\sin \varphi_c + \sin \psi_c)\mathrm{ctg}\, \theta], \quad [7]$$

where θ, φ_c, and ψ_c are the angles at which the film, bubble, and external meniscus surfaces meet the plane $z = z_c$ (see Fig. 4). In this section we will summarize the pertinent equations and will show how φ_c and ψ_c can be calculated from the measured values of r_c, R, and R_f.

Since the film is part of a sphere (see Part I) θ is obtained directly from r_c and R_f:

$$\sin \theta = r_c/R_f. \quad [8]$$

Equations for the shape of the surfaces of the bubble and the external meniscus were derived in Part II in terms of the small parameters

$$\beta = \frac{\Delta\rho g}{\sigma} b^2 \quad \text{and} \quad \epsilon = \sqrt{\frac{\Delta\rho g}{\sigma}}\, r_c \quad [9]$$

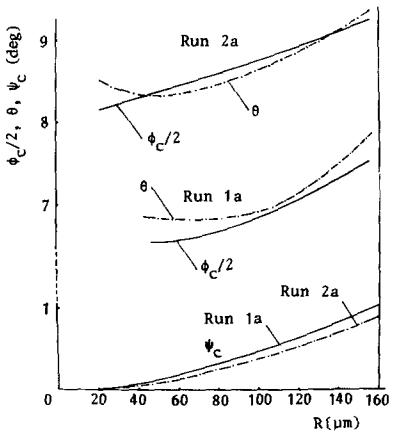

FIG. 4. Calculated values of the angles θ, φ_c, and ψ_c, at which the film, the lower bubble surface, and the external meniscus meet the plane of the contact line for Runs 1a (0.25 kmole/m^3) and 2a (0.32 kmole/m^3).

where b is the radius of curvature at the bottom of the bubble (at $z = 0$), g is the gravity acceleration, and $\Delta\rho$ is the density difference between the liquid and the gas phase. In our experiments ($b \approx R \leqslant 150$ μm and $r_c \leqslant 50$ μm) $\beta < 8 \times 10^{-3}$ and $\epsilon < 3 \times 10^{-2}$. This allows obtaining all numerical results by iterational procedures. The quantities b and β (see Eq. [9]) are calculated from the measured value of R from Eq. [15] of Part II (Ref. (8)):

$$\frac{1}{b} = \frac{1}{R}\left[1 - \frac{\beta}{6} + \frac{\beta^2}{6}(\ln 2 - \tfrac{1}{6})\right] \quad [10]$$

using as zeroth approximation $b^{(0)} = R$. With this result for β one calculates φ_c from Eq. [13] of Part II (where $x(\varphi_c) \equiv r_c$):

$$\sin \varphi_c = \frac{r_c}{b} - \beta\left(\tfrac{1}{3}\,\mathrm{ctg}\,\frac{\varphi_c}{2} - \tfrac{1}{6}\sin 2\varphi_c - \tfrac{1}{2}\sin \varphi_c\right) - \beta^2\left[\left(\tfrac{3}{4} + \tfrac{1}{2}\cos \varphi_c - \tfrac{2}{9}\sin^2\varphi_c - \tfrac{1}{3}\ln \sin \frac{\varphi_c}{2}\right)\sin \varphi_c - \tfrac{1}{2}\left(1 + \tfrac{1}{9}\,\mathrm{ctg}^2\,\frac{\varphi_c}{2}\right)\mathrm{ctg}\,\frac{\varphi_c}{2}\right] \quad [11]$$

using $\varphi_c^{(0)} = \arcsin(r_c/b)$ as zeroth approximation.

Since ψ_c is connected with φ_c, we need a relationship between these quantities. It is provided by the condition for the constancy of the pressure differences between all points of two horizontal planes situated in the bulk gas and liquid phases (13). Applied to $x = 0$ (along the bubble axis) and to $x \to \infty$ (horizontal liquid surface) this condition yields (see Fig. 3 for notations)

$$\frac{2\gamma}{R_f} - \frac{2\sigma}{b} = \Delta\rho g L. \qquad [12]$$

Since $L = z_c - h_c$, where $z_c = z(\varphi_c)$, Eq. [12] along with Eqs. [6], [8] and [9], leads to the sought relationship between ψ_c and φ_c:

$$\sin\psi_c = \frac{r_c}{b}\left[1 + \frac{\beta}{2b}(z_c - h_c)\right] - \sin\varphi_c. \qquad [13]$$

In this equation z_c and h_c must be expressed through Eqs. [14] and [71] of Ref. (8) (with the precision we need the term with ϵ^2 in the latter equation can be left out):

$$z_c \equiv z(\varphi = \varphi_c) = b\left[1 + \cos\varphi_c + \beta\left(\tfrac{1}{3}\sin^2\varphi_c + \tfrac{2}{3}\ln\sin\frac{\varphi_c}{2} - \frac{1 + \cos\varphi_c}{2}\right)\right], \qquad [14]$$

$$h_c = r_c\sin\psi_c \ln\frac{4}{\gamma_e\sqrt{\Delta\rho g/\sigma}\, r_c(1 + \cos\psi_c)} \qquad [15]$$

where $\gamma_e = 1.781\,072\,418\,\cdots$ is Euler's number. The zeroth approximation to be used in [13] when calculating ψ_c is $h_c = 0$, i.e., $\psi_c^{(0)} = 0$. A simplified form of [13] is obtained by neglecting $h_c \ll z_c$, substituting r_c/b and z_c/b from Eqs. [11] and [14], and retaining in the result only the terms linear with respect to β:

$$\sin\psi_c = \frac{\beta}{3}\left(\operatorname{ctg}\frac{\varphi_c}{2} + \tfrac{1}{4}\sin 2\varphi_c\right). \qquad [16]$$

The latter equation yields values of ψ_c slightly higher than those calculated from the more accurate Eq. [13] but it is still useful for error calculations (see the Appendix) and rough estimates.

The set of Equations [6–11] and [13] allows the calculation of film and line tensions γ and κ only from the experimental values of r_c, R, and R_f at a given moment t without making any additional hypothesis. The only assumption that was tacitly made was that the bubble surface and the external meniscus have the same surface tension, σ.

The data from Refs. (14, 15) allowed us to calculate that the change of surface tension due to the increased gas pressure inside the bubble cannot exceed 0.02 mN/m. The curvature effects on σ according to the Gibbs–Tolman–Buff equation (see e.g. (16)) will be of the order of $\Delta\sigma \approx 2\sigma\delta_\infty/R$. Even if one takes $\delta_\infty = 1$ nm, $\Delta\sigma$ will never exceed 2.5×10^{-3} mN/m in our experiments. Possible dynamical changes of the surface tension, caused by the shrinking of the bubble, will be discussed in Section 4.

4. RESULTS AND DISCUSSION

The experiments described in the present paper and more particularly, the data processing, are very much time consuming. Besides, the computation of the final results requires a full series of photographs—the smallest perturbation during the measurement would compromise the whole experiment. Since our major aim was to demonstrate the reliability of the method and to draw attention to some new effects, we have processed in full details only 4 experiments—two for the solution with 0.25 kmole/m^3 NaCl (runs 1a and 1b) and two for 0.32 kmole/m^3 NaCl (runs 2a and 2b). The results are presented on Figs. 5 and 6.

The most striking features in the behavior of $\gamma/2\sigma$ vs P_c are the large variations of γ (the respective values $\gamma_\infty/2\sigma$ for planar films, taken from (11) are shown on the figure) and the fact that at some capillary pressures γ is larger than 2σ, a fact which has not been observed with planar films. Even more interesting are the data for κ (Fig. 6)—besides the large values of κ and the variation of κ with r_c, we must point out to the change of sign of κ for both solutions

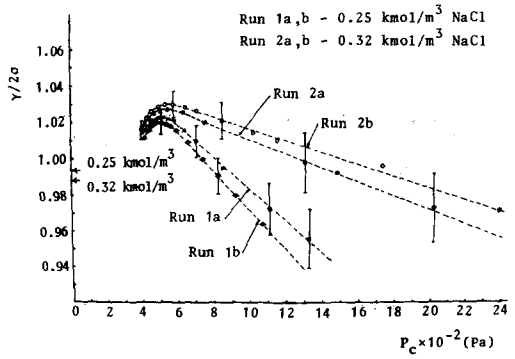

FIG. 5. Dimensionless film tension $\gamma/2\sigma$ vs capillary pressure P_c. The arrows at the ordinate axis denote the values of $\gamma/2\sigma$ for planar films measured in (11) for the respective electrolyte concentrations.

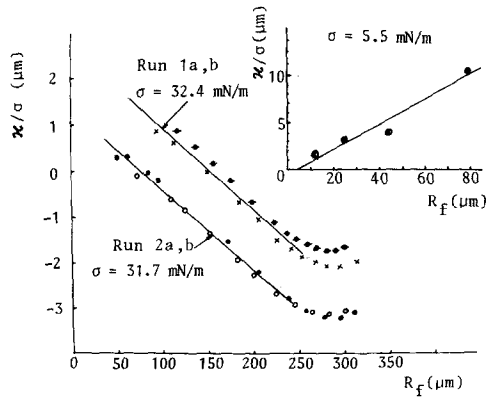

FIG. 7. Dependence of κ/σ vs R_f (the points correspond to Runs 1a (×), 1b (-●-), 2a (○), and 2b (●)). The inset shows the same plot of the data of Torza and Mason (1) for doublets of emulsion droplets.

of NaCl and to the smaller absolute values of κ for smaller bubbles, i.e., for larger r_c^{-1}. There is a tendency of κ to level off for large bubbles ($r_c^{-1} \to 0$), which is more pronounced on the plot κ/σ vs R_f (Fig. 7). An interesting feature of the latter dependence is the fact (which we cannot explain so far) that the slopes of the straight parts of the curves are the same.

All these findings reveal that (unlike the surface tension and similarity to the disjoining pressure) neither γ nor κ depend only on the composition of the solution. On the contrary, they are strong functions of the geometrical parameters of the system. This is a new and unexpected result for γ. For the line tension this was predicted on theoretical grounds by many authors (17, 18, 2, 19) but was not observed so far experimentally.

One way of checking the reliability of our results is to find the limiting values of γ and κ for very large bubbles. Unfortunately because of optical limitations our method cannot be applied to bubbles with radii $R > 160$ μm. Hence, we attempted an extrapolation in coordinates $\kappa/\gamma r_c$ vs r_c^{-1} (see the lower part of Fig. 8) where the tendency is more pronounced. Since κ and γ must reach constant values at $r_c \to \infty$, $\kappa/\gamma r_c$ must go to zero. That is why we connected with the dashed line the last few experimental points with the zero of the coordinate system and drew a parallel line through the respective points of the plot $2\sigma/\gamma$ vs r_c^{-1} (upper part of Fig. 8). The result $2\sigma/\gamma = 1.012$ and the value of the respective contact angle 8.8° agree fairly well with de Feijter's (11) values for planar films[2]: 1.0115 and 8.66°. The same procedure, applied to the data for 0.25 kmole/m^3, gave $2\sigma/\gamma_\infty = 1.007$ and contact angle 6.7° which compare well with de Feijter's findings for the same concentration: 1.0066 and 6.56°, respectively. Without being

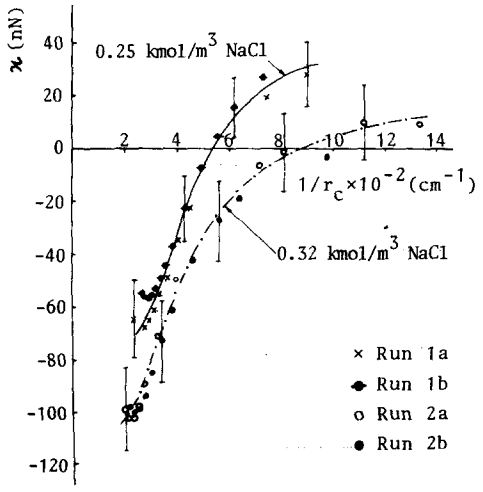

FIG. 6. Line tension, κ, vs reciprocal radius r_c^{-1} of the contact line.

[2] Since de Feijter did not work at 0.32 kmole/m^3 NaCl, the above values were obtained by interpolation between his values for 0.30 and 0.35 kmole/m^3.

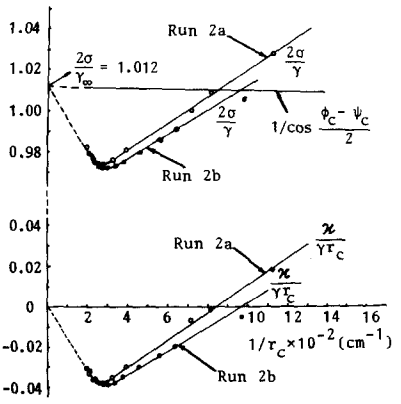

FIG. 8. Plots of the three terms in Eq. [20]: $1/\cos[(\varphi_c - \varphi_c)/2]$, $2\sigma/\gamma$, and $\kappa/\gamma r_c$ vs r_c^{-1} for the solution with 0.32 kmole/m^3 NaCl. The dashed lines denote the extrapolation toward $r_c^{-1} = 0$ (see the text).

a proof, this coincidence is an indication in favor of the correctness of our measurements.

For the time being we are unable to explain the variations of γ with P_c. What can be affirmed is that it is not a simple effect like the dependence of the film tension of a spherical film (20) or of a planar film (21) on the capillary pressure (similar to the dependence of the surface tension on the drop radius): indeed, if it were so the derivative $\partial\gamma/\partial P_c$ should have been of the order of the film thickness, whereas from the steep parts of the plots in Fig. 5 one finds much larger values (around 7.0 μm for 0.25 kmole/m^3 NaCl and 2.5 μm for 0.32 kmole/m^3 NaCl).

There are only a few attempts for experimental determination on the line tension for fluid systems with configuration similar to that of our system. Navascues and Mederos (22) have determined κ from the nucleation rate of water drops on mercury. They found κ *varying* from -2.90×10^{-10} to -3.93×10^{-10} N for critical radii changing from 20.7 to 25.2 nm. These low values of κ should not be surprising in view of the small size of the nuclei. Measurements with particle size close to ours were carried out by Torza and Mason (1), who determined κ from the equilibrium configurations of five doublets of emulsion droplets. They obtained five diffferent values for κ (all of them of the order of 10^{-8} N) and attributed these differences to scattering caused by impurities in their system. In fact, a closer inspection of their data reveals that the variation in κ may well be due to geometrical factors. Indeed, their radius of curvature r_{13} of the interface between the two droplets corresponds to R_f in our experiments and if one plots their data for κ vs R_f (except the point with negative κ, which is obviously erroneous) one obtains a quite good linear dependence (see the inset in Fig. 7), whose slope $\Delta\kappa/\Delta R_f = 0.75$ mN/m by absolute value is close to the slope 0.56 mN/m obtained from our experiments for the same dependence (Fig. 7).

A rigorous thermodynamic theory of the line tension of nonsymmetric curved films will be published soon (the published theories deal with planar films formed in a biconcave meniscus (23, 24, 18). However Churaev *et al.* (2, 3) have performed model calculations of κ for a system to some extent geometrically similar to ours: a sessile spherical drop in equilibrium with a planar thin film. Being well aware of the danger of comparing these two quite different systems, we will nevertheless try to analyze our data using their theory. Churaev *et al.* have adopted the simplified disjoining pressure isotherm shown on the inset in Fig. 9 with the following parameters (2): $\Pi_1 = 10^6$

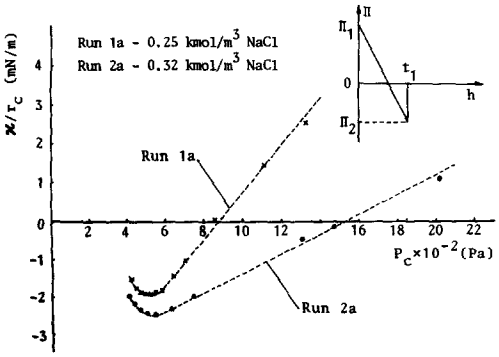

FIG. 9. Plot of κ/r_c vs capillary pressure P_c. Note the existence of linear portions of the curves as required by Eq. [19]. The inset shows the simplified dependence of the disjoining pressure II on the distance h between the interacting surfaces, used by Churaev *et al.* (2, 3).

Pa, $\Pi_2 = -3 \times 10^6$ Pa, $t_1 = 5 \times 10^{-9}$ m, $a = (\Pi_1 - \Pi_2)/t_1 = 8 \times 10^{14}$ Pa/m. Their formula reads (2)

$$\kappa/r_c = -(P_c - \Pi_2)^2/2a + P_c t_1 + \sigma\{1 - [1 + (P_c - \Pi_2)^2/a\sigma]^{1/2}\}. \quad [17]$$

They analyzed only the limiting case $\kappa/r_c = P_c t_1$ following from [17] for the case of very little drops. Instead, for large drops we will expand the square root in [17] in series to obtain

$$\kappa/r_c = P_c t_1 - 3(P_c - \Pi_2)^4/8a^2\sigma. \quad [18]$$

Taking the values of a and Π_2 from (2), we obtain from [18] (for all P_c of our measurements and $\sigma \approx 32$ mN/m) $\kappa/r_c \approx -1.5$ mN/m. At $r_c = 30$ μm this yields $\kappa = -45$ nN which is very close to what we have measured. We deem, however, this numerical coincidence fortuitous, because $|\Pi_2| = 3 \times 10^6$ Pa seems too high and $t_1 = 5 \times 10^{-9}$ m seems too low for foam films.

More important is the functional dependence of κ/r_c on the capillary pressure, P_c, ensuing from [18]. For small P_c one can assume $P_c \ll |\Pi_2|$ and by expanding the second term in [18]. In series one obtains

$$\kappa/r_c \approx (t_1 + 3\Pi_2^3/2a^2\sigma)P_c - 3\Pi_2^4/8a^2\sigma. \quad [19]$$

Hence there should be a range of capillary pressures where κ/r_c is a linear function of P_c. Indeed, our data for κ/r_c plotted in Fig. 9 as a function of P_c exhibit large linear portions. Hence, our results are in *qualitative* agreement with the theory of Churaev, Starov, and Derjaguin. Unfortunately no quantitative comparison of the theory and the experiment is possible, because Eq. [19] contains three unknown parameters: t_1, Π_2, and a.

The correlation between the theory of Churaev, Starov, and Derjaguin and our experimental results is encouraging but nothing more than this. Although the theory predicts the change of sign of κ and the linear dependence of κ/r_c on P_c it is unable to explain (at least in its present form) the deviation of κ/r_c vs P_c from linearity for large bubbles (at $P_c < 6 \times 10^2$ Pa). This was to be expected in view of the crudeness of the model, the approximations, done when deriving Eq. [17], and the difference (including in the geometry) between the systems studied in (2, 3) and in the present work.

Moreover, we cannot for the time being completely rule out the possibility that the observed facts are due, at least in part, to nonequilibrium phenomena such as hydrodynamic resistance preventing the transition region from acquiring its equilibrium shape or local deviations of the surface tension from its equilibrium value. Another nonequilibrium effect may be connected with the relatively slow surfactant desorption during the shrinking of the bubble, which can lead to a change of the surface tension of the lower part ($z < z_c$ in Fig. 3) of the bubble to another value, σ_b. If we knew σ_b, we could calculate the "true" values γ_t and κ_t of the film and line tensions from the equations (cf. Eqs. [6] and [7])

$$\gamma_t \sin\theta = \sigma_b \sin\varphi_c + \sigma \sin\psi_c,$$

$$\gamma_t \cos\theta + \kappa_t/r_c = \sigma_b \cos\varphi_c + \sigma \cos\varphi_c. \quad [20]$$

These equations, along with Eqs. [6] and [7] lead to

$$\gamma - \gamma_t = (\sigma - \sigma_b)\sin\varphi_c/\sin\theta,$$

$$(\kappa - \kappa_t)/r_c = (\sigma - \sigma_b)\sin(\theta - \varphi_c)/\sin\theta.$$

In this case γ and κ (the values plotted in Figs. 5 and 6) must be considered as "apparent" quantities. Let us suppose that the variations of γ and κ are due solely to this effect so that $\gamma_t \equiv \gamma_\infty$. Since σ_b is likely to be smaller than σ, one could explain in this way only the rise of γ for large bubbles whereas this effect is expected to be more efficient for small bubbles. Besides, the numerical estimates showed that the diffusion rate is large enough to make the surface tension difference $\sigma - \sigma_b$ negligibly small. Hence, in spite of being possible this effect can hardly explain the values of γ and κ measured in the present work. The definitive answer to this question requires, however, additional theoretical and experimental studies which are now under way—see, e.g. (25, 26).

Whatever the origin of the effects observed by us might be, we believe we have firmly established that the attachment of small bubbles to a liquid surface gives rise to unexpectedly large line tensions accompanied with corresponding variations of the film tension. Both effects are pronounced functions of the bubble and film radii. These results indicate that the conditions for equilibrium of a fluid particle at another interface are much more complicated than it was believed until now. This conclusion will remain valid even if the line and film tension effects turn out to be determined by nonequilibrium phenomena as discussed above. Indeed, the shrinking of the bubble is an irreversible process, controlled by the slow diffusion of gas through the film. Hence this system is a nonequilibrium one with respect to the *chemical* (diffusive) equilibrium, but *thermal,* and *mechanical* equilibrium should exist during this process. So, γ and κ must be considered as parameters of the system, which are defined by the conditions for *mechanical* equilibrium.

Scheludko, Platikanov, and co-workers (4–6) have studied the same system as us (in a wider range of electrolyte concentrations) but have obtained very different results: e.g., for 0.32 kmole/m^3 NaCl they found a constant value $\kappa = +0.85$ nN. In (5, 6) these authors also used Princen and Mason's method (10) of the shrinking bubble (they called it "the diminishing bubble method") in conjunction with one projection of the force balance equations of Pujado and Scriven (27). The approximate equation they used follows also from our Eq. [60] in Part I if one neglects the second and third terms under the square root:

$$\frac{1}{\cos(\alpha/2)} = \frac{2\sigma}{\gamma} - \frac{\kappa}{\gamma r_c}, \qquad [21]$$

where $\alpha = \phi_c - \psi_c$. Since these authors did not use a second force balance equation and have not measured R_f, they tacitly replaced the missing experimental information by the hypothesis that both γ and κ should not depend on r_c, i.e., that $1/\cos(\alpha/2)$ should be a linear function of r_c^{-1}. Our Fig. 8 shows that the opposite is true: $\cos(\alpha/2)$ remains almost constant whereas the large variations of $2\sigma/\gamma$ and $\kappa/\gamma r_c$ compensate each other. This is confirmed also by the plot of $1/\cos(\alpha/2)$ vs $1/r_c$ on Fig. 10. (Note that α is calculated by using the data only for the two radii R and r_c, measured directly.) The pronounced curvature reveals that neither γ, nor κ in Eq. [21] is constant. The same conclusion follows from the data of Platikanov *et al.* (5)—see the inset on Fig. 10, calculated by us from the data of their Fig. 3 by means of their Eq. [9]. In fact these authors noticed the curvatuve of the dependence of $1/\cos(\alpha/2)$ vs $1/r_c$ and interpreted it correctly as an indication that both γ and κ are functions of the capillary pressure, i.e., of the bubble radius. They neglected however this fact when processing their data. They plotted on the same figure the data for several bubbles and since the data were scattered, obtained a cloud of points. Although the dependence of $1/\cos(\alpha/2)$ vs $1/r_c$ for every *single* bubble was curvilinear, they drew a straight line through the cloud of points for the assembly of bubbles. We believe that such a procedure is not correct.

Therefore, the basic assumption, used in (5, 6) to calculate κ, is not confirmed. The so-called "critical bubble method" (4) is based on similar assumptions. It is then understandable why the values of κ, obtained in (4–6) by means of these methods, disagree with our experimental findings.

5. CONCLUDING REMARKS

The most important results of the present study is the finding that the film tension γ and the line tension κ strongly depend on the geometrical parameters of the system. Beside, the line tension turned out to be much larger by absolute value than previously reported by Scheludko *et al.* (4–6) and had a predominantly negative sign. Its absolute value reveals a tendency to decrease with the bubble radius and to level off for relatively large bubbles. The extrapolated values for γ are in good agreement with those measured by de Feijter

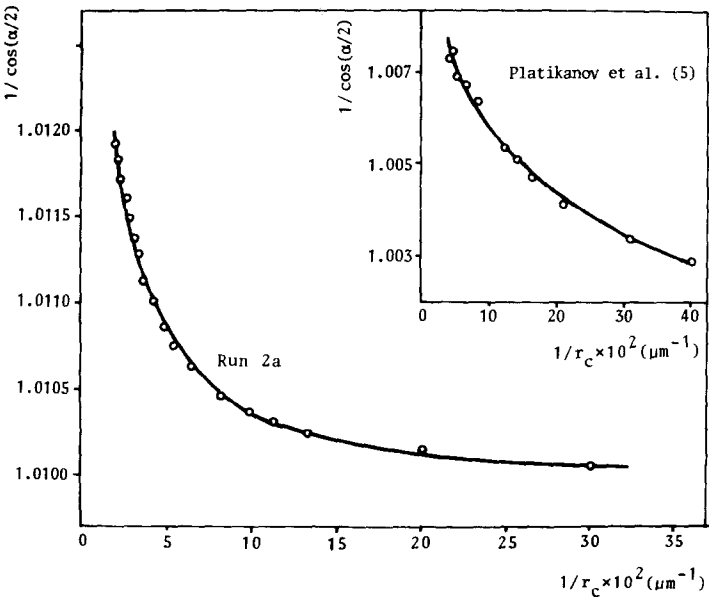

FIG. 10. The data from Run 2a (0.32 kmole/m^3 NaCl at 22°C) in the scale $1/\cos(\alpha/2)$ vs $1/r_c$. The inset shows the same plot, obtained from the data of Platikanov *et al.* (5) for the same solution at 25°C.

(11) for large films. The line tensions measured by us are similar to those found by Torza and Mason (1) in their dependence on the film radius and are of the same order of magnitude. They are also in agreement with the theory of Churaev, Starov, and Derjaguin (2, 3). Nevertheless, for the time being we can not completely rule out the possibility that the effects observed by us are at least in part due to nonequilibrium effects. The discrepancy between our results and those of Scheludko, Platikanov, and co-workers (4–6) is due to the fact that those authors have used the assumption that the film and line tensions do not depend on the corresponding radii of curvature.

APPENDIX: ERROR CALCULATIONS

When a new effect is found experimentally, one must make sure that it is larger than the error involved in the measurements and the calculations. Hence, we describe briefly the way in which we have calculated the errors ΔY of the measured quantities Y. The latter can be divided into two groups: basic quantities (r_c, R, and R_f), that are randomly distributed and quantities that are calculated (φ_c, ψ_c, θ, $\gamma/2\sigma$, and κ/σ) from analytical equations using the measured values of r_c, R, and R_f. For the first group one has (28)

$$\Delta Y = \left[\frac{\Phi_{\min}}{n(n-m)}\right]^{1/2} \qquad [22]$$

where $\Phi_{\min}$ is the minimum value of Φ as defined for R by [2] and by analogous expressions for r_c and R_f (see Section 2), n is the number of the experimental points, and m is the number of parameters that have been varied when minimizing the Φs. If $Y = Y(x_1, x_2, \cdots)$ is the equation used to calculate a given quantity Y from the second group, its error will be

$$\Delta Y = \left[\left(\frac{\partial Y}{\partial x_1}\Delta x_1\right)^2 + \left(\frac{\partial Y}{\partial x_2}\Delta x_2\right)^2 + \cdots\right]^{1/2} + (\Delta Y)_e \qquad [23]$$

where Δx_1, Δx_2, $\cdots$ are the errors of the independently measured parameters and $(\Delta Y)_e$ is the error of the equation used when it is approximated. When the equation is exact $(\Delta Y)_e \equiv 0$.

TABLE I

Standard Deviations of R_f, R, and r_c Calculated from Eq. [22]

	Data for R_f, $m = 2$			Data for R, $m = 4$			Data for r_c, $m = 3$		
Run	n	Φ_{min} (μm^2)	ΔR_f (μm)	n	Φ_{min} (μm^2)	ΔR (μm)	n	Φ_{min} (μm^2)	Δr_c (μm)
1a	12	27.65	0.48	24	6.28	0.11	17	3.74	0.13
1b	14	112.96	0.82	33	2.60	0.05	23	5.52	0.11
2a	11	93.06	0.94	19	4.44	0.12	15	3.13	0.13
2b	12	288.30	1.55	23	2.87	0.08	17	4.03	0.13

In Table I we have presented the data used and the results from the calculations by Eq. [22].

The error introduced by the terms with β and β^2 in Eq. [11] are negligible, so that

$$\Delta(\sin\varphi_c) = \left[\left(\frac{\Delta r_c}{R}\right)^2 + \left(\frac{r_c \Delta R}{R^2}\right)^2\right]^{1/2} + \frac{4}{225}\beta^3 \mathrm{ctg}^5\frac{\varphi_c}{2}$$

where the last term is the error $(\Delta\varphi_c)_e$ of the asymptotic equation (see Part II). One can neglect the errors introduced in $\Delta\psi_c$ by the second term in the parenthesis in Eq. [16] and by $(\Delta\psi_c)_e$, so that (see also [13]):

$$\frac{\Delta \sin\psi_c}{\sin\psi_c} = \left[\left(\frac{\Delta\rho}{\rho}\right)^2 + \left(\frac{\Delta\sigma}{\sigma}\right)^2 + \left(\frac{2\Delta R}{R}\right)^2 + \left(\frac{\Delta\varphi_c}{\sin\varphi_c}\right)^2\right]^{1/2}.$$

The quantities θ, $\gamma/2\sigma$, and κ/σ are calculated from the exact equations [8], [6], and [7]. Therefore, according to [23], their errors wil be

$$\Delta\theta = \frac{1}{\cos\theta}\left[\left(\frac{\Delta r_c}{R_f}\right)^2 + \left(\frac{r_c \Delta R_f}{R_f^2}\right)^2\right]^{1/2},$$

$$\Delta\left(\frac{\gamma}{2\sigma}\right) = \tfrac{1}{2}\left\{\left(\frac{\Delta \sin\varphi_c}{\sin\theta}\right)^2 + \left(\frac{\Delta \sin\psi_c}{\sin\theta}\right)^2 + \left[\frac{\Delta \sin\theta}{\sin^2\theta}(\sin\varphi_c + \sin\psi_c)\right]^2\right\}^{1/2}$$

$$\Delta\left(\frac{\kappa}{\sigma}\right) = r_c\left\{\left(\frac{\kappa \Delta r_c}{\sigma r_c^2}\right)^2 + [(\sin\varphi_c + \cos\varphi_c \mathrm{ctg}\,\theta)\Delta\varphi_c]^2 + [(\sin\psi_c + \cos\psi_c \mathrm{ctg}\,\theta)\Delta\psi_c]^2 + \left[\left(\sin\varphi_c + \sin\psi_c\right)\frac{\Delta\theta}{\sin^2\theta}\right]^2\right\}^{1/2}.$$

ACKNOWLEDGMENTS

The authors are indebted to Dr. Zh. Zheljazkov for the computer calculations, to E. Basheva for preparing of the manuscript, to Referee II, Dr. J. A. de Feijter, and Dr. M. Vignes-Adler for their valuable comments.

REFERENCES

1. Torza, S., and Mason, S. G., *Kolloid-Z. Z. Polym.* **246,** 593 (1971).
2. Starov, V. M., and Churaev, N. V., *Kolloidn. Zh.* **42,** 703 (1980).
3. Churaev, N. V., Starov, V. M., and Derjaguin, B. V., *J. Colloid Interface Sci.* **89,** 16 (1982).
4. Platikanov, D., Nedyalkov, M., and Scheludko, A., *J. Colloid Interface Sci.* **75,** 612 (1980).
5. Platikanov, D., Nedyalkov, M., and Nasteva, V., *J. Colloid Interface Sci.* **75,** 620 (1980).
6. Scheludko, A., Toshev, B. V., and Platikanov, D., *in* "The Modern Theory of Capillarity" (F. C. Goodrich and A. I. Rusanov, Eds.). Akademie-Verlag, Berlin, 1981.
7. Ivanov, I. B., Kralchevsky, P. A., and Nikolov, A. D., *J. Colloid Interface Sci.* **112,** 97 (1986).
8. Kralchevsky, P. A., Ivanov, I. B., and Nikolov, A. D., *J. Colloid Interface Sci.* **112,** 108 (1986).
9. Nikolov, A. D., Kralchevsky, P. A., and Ivanov, I. B., *J. Colloid Interface Sci.* **112,** 122 (1986).
10. Princen, H. M., and Mason, S. G., *J. Colloid Sci.* **20,** 353 (1965).
11. De Feijter, J. A., thesis. University of Utrecht, 1973;

De Feijter, J. A., and Vrij, A., *J. Colloid Interface Sci.* **64,** 269 (1978).
12. Padday, J. F., *in* "Surface and Colloid Science" (E. Matijevic, Ed.), Vol. 1, p. 101. Wiley, New York, 1969.
13. Princen, H. M., *J. Colloid Sci.* **18,** 178 (1963).
14. Massoudi, R., and King, A. D., *J. Phys. Chem.* **78,** 2262 (1974).
15. Massoudi, R., and King, A. D., *J. Phys. Chem.* **79,** 1670 (1975).
16. Ono, S., and Kondo, S., "Handbuch der Physik," Vol. 10. Springer-Verlag, Berlin, 1958.
17. Rusanov, A. I., *Kolloidn. Zh.* **39,** 704 (1977).
18. Ivanov, I. B., Toshev, B. V., and Radoev, B. P., *in* "Wetting, Spreading and Adhesion" (J. F. Padday, Ed.), p. 37. Academic Press, New York, 1978.
19. Navascues, G., and Tarazona, P., *Chem. Phys. Lett.* **82,** 586 (1981).
20. Rusanov, A. I., *in* "Surface Forces and Liquid Interfaces" (B. V. Derjaguin, Ed.), p. 158. Nauka, Moscow, 1983 [in Russian].
21. Ivanov, I. B., and Toshev, B. V., *Colloid Polym. Sci.* **253,** 593 (1975).
22. Navascues, G., and Mederos, L., *Surf. Technol.* **17,** 79 (1982).
23. De Feijter, J. A., and Vrij, A., *J. Electroanal. Chem. Interfacial Electrochem.* **37,** 9 (1972).
24. Martynov, G. A., Ivanov, I. B., and Toshev, B. V., *Kolloidn. Zh.* **38,** 474 (1976).
25. Kralchevsky, P. A., Ivanov, I. B., *Chem. Phys. Lett.* **121,** 111 (1985).
26. Kralchevsky, P. A., Ivanov, I. B., *Chem. Phys. Lett.* **121,** 116 (1985).
27. Pujado, P. R., and Scriven, L. E., *J. Colloid Interface Sci.* **40,** 82 (1972).
28. Sveshnikov, A. A., "Principles of Error Theory," p. 113. Leningrad University, Leningrad, 1972 [in Russian].